DOI: 10.1002/ejoc.200600299

Complete Chiral Induction from Enantiopure 1,2-Diamines to Benzophenone-Based Achiral Bisphosphane Ligands in Noyori-Type Ru^{II} Catalysts

Qing Jing,[a] Christian A. Sandoval,[a] Zheng Wang,[a] and Kuiling Ding*[a]

Keywords: Asymmetric catalysis / Chiral induction / Diamine / Hydrogenation / Ketone / Benzophenone / Bisphosphane / Ruthenium

We report the design and synthesis of a novel class of Ru^{II} catalysts (**3**) composed of achiral benzophenone-based bisphosphane ligands and enantiopure 1,2-diamines for the asymmetric hydrogenation of aryl ketones. The developed catalysts show excellent enantioselectivities (up to 97 % *ee*) and activities (up to S/C = 10,000) in the hydrogenation of a variety of aromatic ketones. Complete chiral induction from the enantiopure 1,2-diamine to the achiral bisphosphane ligand was observed. The coordination of the C=O moiety in **3** to the cationic Ru^{II} center is considered to be of key importance in providing a higher thermodynamic and kinetic rotation barrier for the flexible bisphosphane ligand, resulting in the preferential formation of only one diastereomer, and thus explaining the high enantioselectivity of the catalyst.

Introduction

Catalytic asymmetric hydrogenation of simple ketones is of fundamental importance in organic synthesis.[1] In general, high catalytic efficiency in terms of reactivity and selectivity is afforded by the presence of a rigid, fixed, and enantiopure ligand framework around the metal centre. The use of Noyori's [$RuCl_2$\{(*R*)-BINAP\}\{(*R*,*R*)-DPEN\}] catalyst **1** [BINAP: 2,2′-bis(diarylphosphanyl)-1,1′-binaphthyl; DPEN: 1,2-diphenylethylenediamine] has provided the most efficient process for the production of optically active secondary alcohols from simple, aromatic prochiral ketones.[1–2] In such systems, chiral bisphosphanes have proven to be the most successful and widely used ligands for this purpose,[2–3] with their high degrees of enantioselectivity being considered to result from the synergistic effect of the chiral diphosphane and chiral diamine ligands.[4] Alternatively, research pioneered by Mikami and Noyori showed the feasibility of using the chirally flexible diphosphane BIPHEP [BIPHEP: 2,2′-bis(diphenylphosphanyl)-1,1′-biphenyl] together with an enantiopure chiral diamine (DPEN) to generate Noyori-type Ru^{II} catalysts (**2**) on the basis of the asymmetric activation concept.[5–6] The resulting complexes demonstrated good to excellent enantioselectivities (63–92 % *ee*s) in the hydrogenation of ketones.[7] In this catalyst system, a 3:1 mixture of (*S*)/(*S*,*S*) and (*R*)/(*S*,*S*) BIPHEP-chelate Ru^{II} diastereomers was observed, with the major isomer also predominating in the catalytic process. Here we report the development of a new type of Ru^{II} catalyst (**3**, Scheme 1) based on enantiopure 1,2-diamine and achiral bidentate benzophenone-based phosphane ligands for the asymmetric hydrogenation of aryl ketones. Complete chiral induction by the chiral 1,2-diamines has been observed for **3**, resulting in the efficient hydrogenation of a variety of aromatic ketones with excellent enantioselectivities (97 % *ee*s).[8]

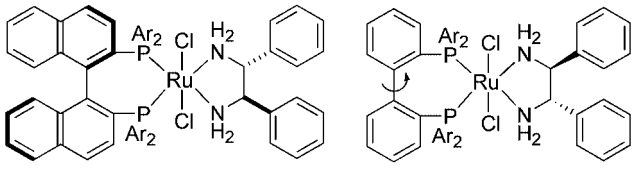

1 **2**

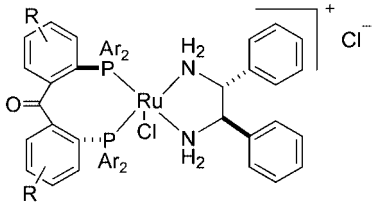

3a: Ar = C_6H_5, R = H
3b: Ar = C_6H_5, R = 5-$C(CH_3)_3$
3c: Ar = C_6H_5, R = 4-$C(CH_3)_3$
3d: Ar = 3,5-$(CH_3)_2C_6H_3$, R = H

Scheme 1.

[a] State Key Laboratory of Organometallic Chemistry, Shanghai Institute of Organic Chemistry, Chinese Academy of Sciences, 354 Fenglin Road, Shanghai 200032, China
Fax: +86-21-6416-6128
E-mail: kding@mail.sioc.ac.cn
Supporting information for this article is available on the WWW under http://www.eurjoc.org or from the author.

Results and Discussion

Benzophenone, although an achiral molecule, has been shown to exist in the solid state in two different enantiomeric forms.[9] This is due to its ability to form right-handed (*M*) or left-handed (*P*), two-winged, propeller-like structures through simple rotation about the (Aryl)CC(C=O) bonds. In the solid state such structures are frozen (Scheme 2). Although the rotational barrier is low at room temperature, benzophenone can in principle offer the potential to act as a chiral backbone in bisphosphane ligand construction, due to this propeller-like structural feature. Furthermore, upon chelation to a metal ion, such a configuration can be frozen out in an analogous manner to benzophenone in the solid state (Scheme 2).

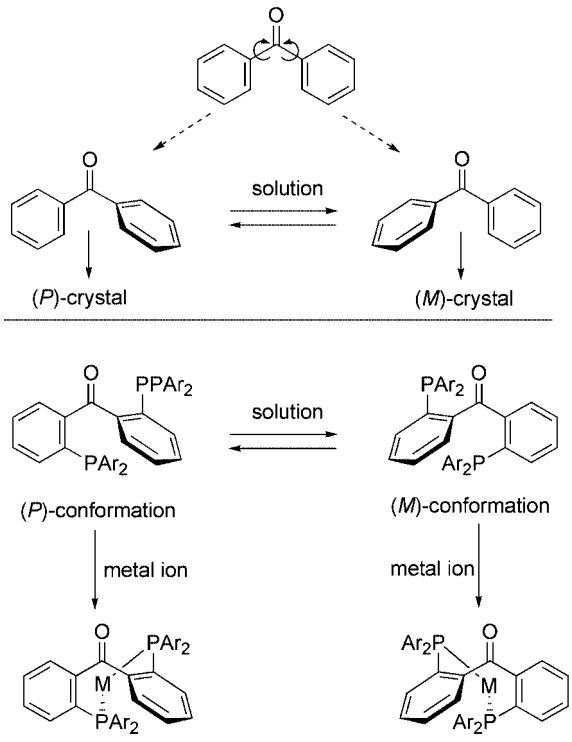

Scheme 2. Schematic representation of chirality for benzophenone in the crystalline state and the chirality of benzophenone-based bisphosphane ligand upon metal complexation.

Ligand Synthesis

With the above in mind, we designed a series of achiral bisphosphane ligands **9**–**10**, each possessing a benzophenone unit as the backbone. The synthesis of these benzophenone-based ligands is quite straightforward. As shown in Scheme 3, addition of Grignard reagents formed from 2-methoxyaryl bromides (compounds **4**) to 2-methoxyarylaldehydes[10] gave the corresponding dihydrobenzophenzone derivatives **5** in good yields (73–84%). Simple oxidation of **5** with $K_2Cr_2O_7$[11] in DMF afforded the corresponding

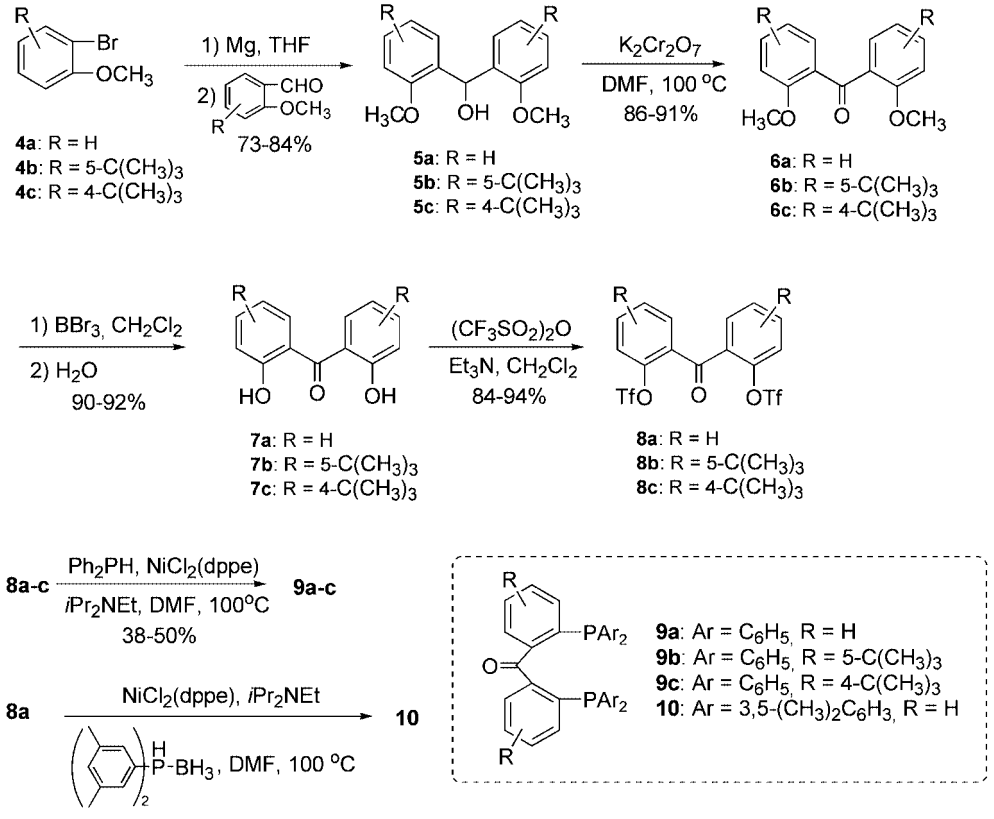

Scheme 3. Synthesis of achiral benzophenone-based bisphosphane ligands.

ketones **6** in yields of 86–91%, demethylation of **6** with BBr_3[12] at –78 °C provided the benzophenone-based diphenols **7** in excellent yields (90–92%), and these in turn conveniently gave the corresponding ditriflate derivatives **8** in high yields (84–94%) upon treatment with trifluoromethanesulfonic anhydride (Tf_2O) in the presence of Et_3N. $NiCl_2$/dppe-catalyzed cross-couplings[13] between **8** and Ph_2PH proceeded smoothly in DMF at 100 °C to afford the target ligands **9** in 38–50% yields, whilst ligand **10**, a structural analogue of **9** with bulkier bis(3,5-xylyl)phosphanyl moieties in its chelating units, was synthesized in 25% yield in a similar procedure, by treatment of **8a** with $(3,5\text{-Xyl})_2PH{\cdot}BH_3$ complex. The ligand **9a** was structurally examined by X-ray diffraction analysis and was confirmed to adopt both right- and left-handed propeller configurations in the solid state (Figure 1, a), although the flexible ligands **9** and **10** exhibit no defined chiral structure in solution, due to inherently very low rotational energy barriers.

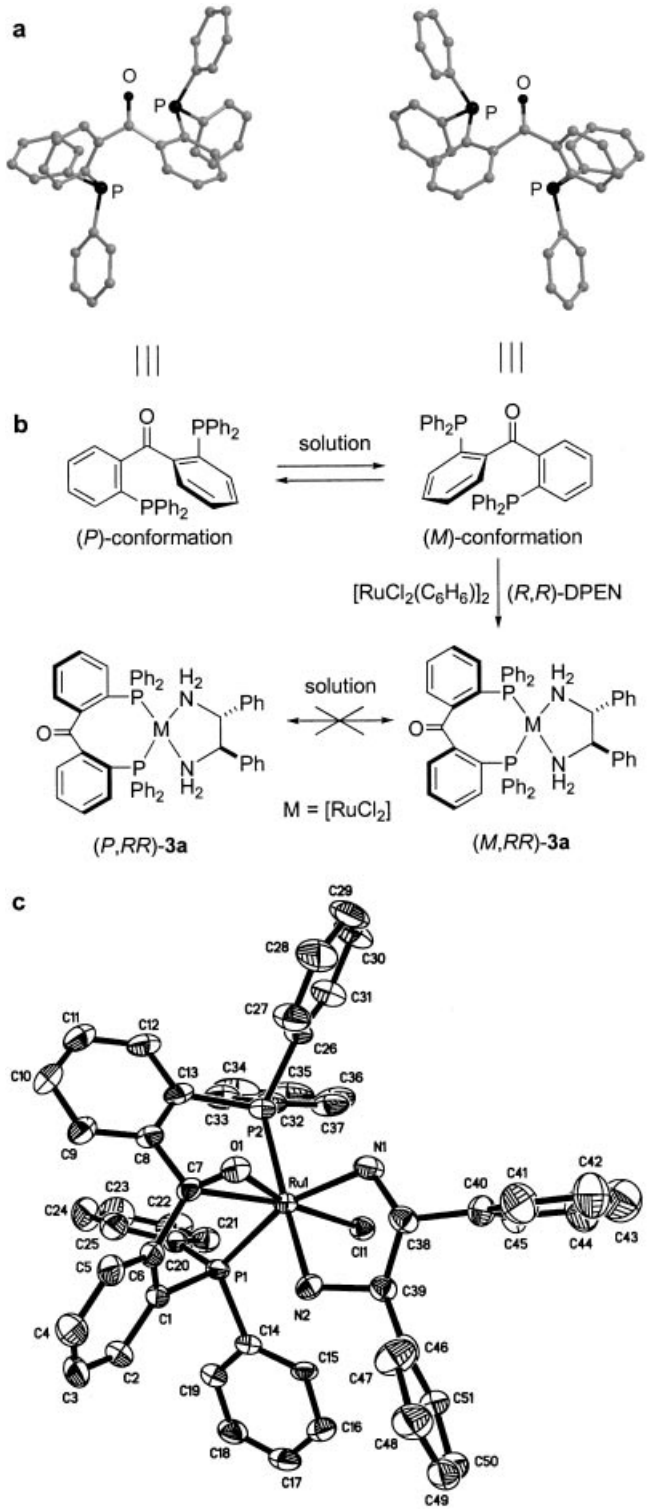

Figure 1. a) Molecular structure of **9a** in (*P*) and (*M*) conformations. b) Enantiocontrol by chiral (*R*,*R*)-DPEN resulting in a preferential homochiral (*M*,*RR*) arrangement about the metal center. c) Crystal structure of (*M*,*RR*)-**3a**.

Catalyst Synthesis and Characterization

The general synthetic route to Ru^{II} catalysts follows a well established procedure reported by Noyori.[2a–2b] Heating of a mixture of phosphane ligand (**9** or **10**) with $[Ru^{II}Cl_2(benzene)]_2$ in DMF at 100 °C for 25 min, followed by addition of the chiral 1,2-diamine (*R*,*R*)-DPEN in CH_2Cl_2, yielded the corresponding complexes **3** in yields of 80–84% (Scheme 4). These precatalysts were stable in air and could be stored for indefinite periods without strict exclusion of moisture or air.

Although the flexible ligands **9** (and **10**) did not adopt defined enantiomeric structures in solution, determination of the single-crystal X-ray structure of **9a** revealed that in the solid state the benzophenone-based ligand adopts a structural motif similar to that of benzophenone. As shown in Figure 1a, the two phenyl rings in the benzophenone backbone of **9a** form a two-winged propeller-like conformation, the dihedral angle between the two benzophenone phenyl rings being 78.82(7)° (56° in benzophenone[9a]). As would be expected from Scheme 2, this propeller-like structural feature is indeed maintained upon complex formation with Ru^{II} metal ion. X-ray structural determination of **3a** revealed that the ligand **9a** adopts a single conformation in the solid state, with a dihedral angle of 74.98(31)° between the benzophenone phenyl rings, so the conformation of chelated ligand **9a** in complex **3a** can be assigned as *M* (right-handed) in an analogous fashion to the case of benzophenone (Scheme 2).

In solution, the ^{31}P NMR spectra for complexes **3a**–**d** each showed a pair of doublets (Table 1) with J_{PP} ranging from 23.0 to 37 Hz, while their ^1H NMR spectra each displayed individual resonances for the 1,2-diphenylethylenediamine moiety. Complexes **3a**–**d** thus have C_1 symmetry in solution, which is consistent with the solid-state structure of **3a**. There was no change in the ^1H NMR spectrum of **3a** over a period of 48 h, indicating no dynamic configurational change in solution. Obviously, complete chiral induction from (*R*,*R*)-DPEN to the benzophenone-based bisphosphane ligand, through the Ru^{II} metal center, has occurred in **3**. This structural feature would be expected to provide an excellent means for enantioselective control in catalytic reactions (Figure 1).

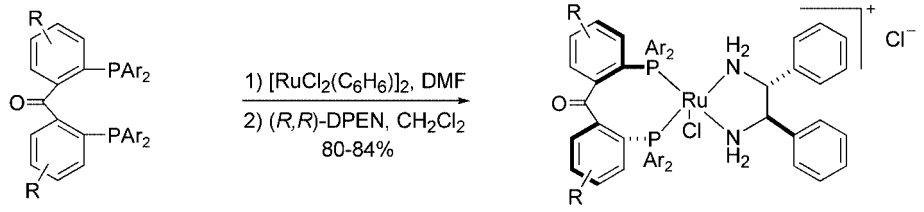

9a: Ar = C_6H_5, R = H
9b: Ar = C_6H_5, R = 5-$C(CH_3)_3$
9c: Ar = C_6H_5, R = 4-$C(CH_3)_3$
10: Ar = 3,5-$(CH_3)_2C_6H_3$, R = H

(*R*,*R*)-**3a**: Ar = C_6H_5, R = H
(*R*,*R*)-**3b**: Ar = C_6H_5, R = 5-$C(CH_3)_3$
(*R*,*R*)-**3c**: Ar = C_6H_5, R = 4-$C(CH_3)_3$
(*R*,*R*)-**3d**: Ar = 3,5-$(CH_3)_2C_6H_3$, R = H

Scheme 4. Synthesis of Ru^{II} complexes **3a**–**d**.

Table 1. ^{31}P NMR chemical shifts (δ, ppm) and IR $\tilde{\nu}_{C=O}$ (cm^{-1}) for Ru complexes **3** and achiral bis-phosphane ligand **9** or **10**.

	^{31}P NMR[a] [δ, ppm]	$J_{P,P}$ [Hz]	$\tilde{\nu}_{C=O}$ [cm^{-1}]	$\Delta\tilde{\nu}_{C=O}$[b] [cm^{-1}]
9a	–7.3 (s)	–	1652	–
3a	47.2 (d), 47.7 (d)	23.0	1665	+13
9b	–7.8 (s)	–	1660	–
3b	46.4 (d), 44.7 (d)	23.2	1667	+7
9c	–6.3 (s)	–	1653	–
3c	47.8 (d), 47.4 (d)	23.4	1669	+16
10	–16.9 (s)	–	1663	–
3d	54.0 (d), 53.2 (d)	37.0	1670	+7

[a] Multiplicity: s = singlet, d = doublet. [b] Difference in $\tilde{\nu}_{C=O}$ between free ligand (**9**, **10**) and the corresponding Ru complex (**3**).

Moreover, the molecular structure clearly shows short distances for the C(7)–Ru [2.144(7) Å] and O(1)–Ru [2.070(5) Å] bonds, indicating a strong agostic bond. Such a (C=O)···Ru^{II} interaction is further demonstrated by the changes in the $\tilde{\nu}_{C=O}$ absorption in the IR spectra of ligands **9**–**10** and their corresponding complexes **3a**–**d** (Table 1). Upon complexation, the $\tilde{\nu}_{C=O}$ absorptions for the ligands are shifted by 7–16 cm^{-1} to shorter wavelengths, indicating strong interaction between the carbonyl group and the Ru^{II} metal center. It is interesting to note that the complex **3a** exists in the solid state as a distinct ion pair: [RuCl(**9a**)((*R*,*R*)-DPEN)]$^+$ and Cl^- (Figure 1, c). This ionic feature and its counterparts can also be observed in the MALDI spectra of **3a**–**d**, with the distinct appearance of [RuCl(**9**)((*R*,*R*)-DPEN)]$^+$ (*m*/*z* = 899) or [RuCl(**10**)((*R*,*R*)-DPEN)]$^+$ (*m*/*z* = 1011) species (see Figure S1 in the Supporting Information). Such properties contrast with those of other analogous bisphosphane or monophosphane Ru^{II} complexes[2a,2b,14] and are attributable to the relatively strong (C=O)···Ru^{II} interaction that facilitates the ionization of Cl^- from the coordination sphere of Ru^{II}. We believe that the coordination of C=O to the cationic complex provides a higher thermodynamic and kinetic rotational barrier for the flexible phosphane ligand in **3**, which thus exists as only one diastereomer in the complex. This point is likely to be very important for the design of enantiopure catalysts with chirally flexible ligands and enantiopure 1,2-diamines.

Asymmetric Hydrogenation of Arylketones Catalyzed by 3a–d

With the complexes **3a**–**d** at hand, the catalyst performance was then investigated with hydrogenation of acetophenone (**11**) as a model reaction. The hydrogenation was carried out in the presence of 0.1 mol-% of **3a**–**d** under 20 atm of H_2 pressure at room temp. As shown in Table 2, the hydrogenation of **11** in the presence of **3a** proceeded efficiently in various alcoholic solvents, including ethanol, *n*-propanol, isopropanol, or *n*-butanol, to give (*S*)-1-phenylethanol [(*S*)-

Table 2. Hydrogenation of acetophenone (**11**) catalyzed by (*R*,*R*)-**3** in various solvents.[a]

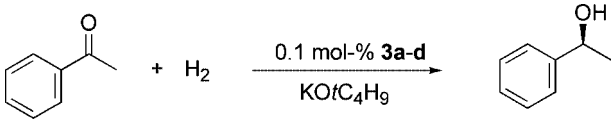

11 (*S*)-**12**

Entry	Catalyst	Solvent	Conv.[b] [%]	*ee*[c] [%]
1	**3a**	MeOH	85	76
2	**3a**	EtOH	>99	90
3	**3a**	*n*-PrOH	>99	89
4	**3a**	*i*-PrOH	>99	81
5	**3a**	*n*-BuOH	>99	89
6	**3a**	*t*-BuOH	NR[d]	–
7	**3a**	DMF	NR[d]	–
8	**3b**	*n*-PrOH	>99	80
9	**3c**	EtOH	>99	88
10	**3c**	*n*-PrOH	>99	86
11	**3c**	*i*-PrOH	>99	81
12	**3d**	EtOH	>99	88
13	**3d**	*n*-PrOH	>99	87
14	**3d**	*i*-PrOH	>99	88
15[e]	**3a**	EtOH	>99	89
16[f]	**3a**	EtOH	57	90
17[g]	**3a**	EtOH	>99	91
18[h]	**3a**	EtOH	>99	91

[a] Conditions: [**3**] = 1.5 mM, [**11**] = 1.5 M (S/C = 1000), [KO*t*Bu] = 30 mM, $P(H_2)$ = 20 atm, *t* = 6 h, *T* = 25 °C. [b] Determined by ^1H NMR spectroscopy. [c] Determined by GC (Supelco BETA-DEX 120). The configuration of **12** determined by $[\alpha]_D$ is (*S*). [d] No product was detected by GC. [e] S/C = 10,000, [**3**] = 0.75 mM, [**11**] = 7.5 M, [KO*t*Bu] = 15 mM, *t* = 12 h. [f] $P(H_2)$ = 10 atm, *t* = 4 h. [g] $P(H_2)$ = 40 atm, *t* = 4 h. [h] $P(H_2)$ = 80 atm, *t* = 4 h.

12] with 81–90% enantiomeric excesses (*ee*s, Entries 2–5). Methanol proved to be a poor solvent in terms both of activity and of enantioselectivity (Entry 1 vs. Entries 2–5). No reaction was observed in *tert*-butyl alcohol or DMF under the same experimental conditions (Entries 6–7). The use of catalysts **3b**–**d** in the hydrogenation of **11** in different alcoholic solvents revealed similar reactivities, though ethanol proved to be optimal in terms of obtained *ee* for (*S*)-**12**. Of the catalysts examined (**3a**–**d**), **3a** showed the best performance in hydrogenating **11** (90% *ee*). When the catalyst loading was reduced to 0.01 mol-% the hydrogenation of **11** still proceeded smoothly without obvious loss of enantioselectivity (Entry 15 vs. 2), demonstrating the high activity of the catalyst system. While the pressure of H_2 did influence the reaction rate (Entry 16),[15] it did not show any obvious impact on the enantioselectivity (Entries 16–18 vs. 2).

Table 3. Hydrogenation of acetophenone (**11**) by catalyst formed in situ from **13** and various chiral 1,2-diamines (**14**–**16**).[a]

Entry	1,2-Diamine	Conversion[b] [%]	*ee*[c] [%]
1	**14a**	>99	90
2	**14b**	>99	58
3	**14c**	>99	77
4	**14d**	>99	88
5	**14e**	>99	89
6	**14f**	>99	80
7	**14g**	>99	87
8	**15**	98	69
9	**16**	>99	82

[a] Conditions: [**13**] = 1.5 mM, [diamine] = 1.8 mM, [**11**] = 1.5 M (S/C = 1000), [KO*t*Bu] = 30 mM, $P(H_2)$ = 20 atm, t = 6 h, T = 25 °C. [b] Determined by ^{1}H NMR spectroscopy. [c] Determined by GC (Supelco BETA-DEX 120). The configuration of **12** determined by $[\alpha]_D$ is (*S*).

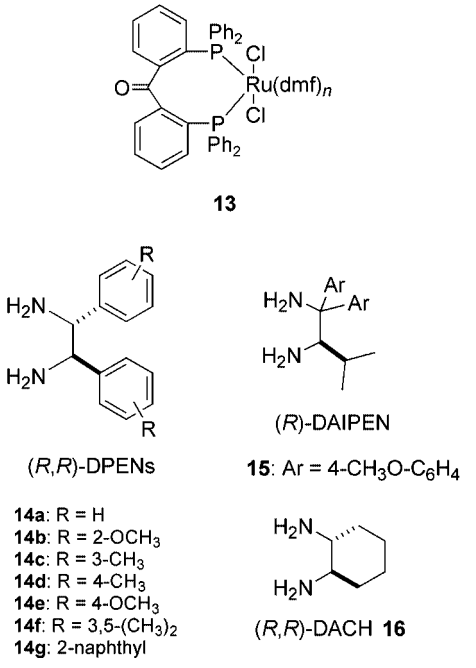

Scheme 5. Generation of Ru^{II} catalysts by in situ mixing of precomplex **13** with various chiral 1,2-diamines.

These results encouraged us to screen several chiral 1,2-diamines for the hydrogenation of **11** with in situ combinations of **9a**/$RuCl_2$ (**13**) under the experimental conditions shown in Entry 2 in Table 2. As shown in Table 3, sterically bulky chiral 1,2-diamines such as **14b**–**c**, **14f**, and **15** are obviously unfavorable for enantiocontrol by the catalysis (Entry 1 vs. Entries 2–3, 6 and 8). The catalysts **14d**–**e** and **14g**, generated by use of more sterically demanding chiral 1,2-diamines, afforded results comparable to those obtained with **14a** (Entry 1 vs. Entries 4–5 and 7), whilst catalysts generated from chiral 1,2-diaminocyclohexane (**16**) afforded moderate enantioselectivity (82% *ee*, Entry 9). Thus, although it might have been expected that more bulkily substituted ligands **14b**–**g** and **15** should have resulted in higher chiral induction,[2] the simple 1,2-diamine **14a** [(*R*,*R*)-DPEN] turned out to be the best under the conditions used (Scheme 5).

Under optimized conditions, a variety of aromatic ketones were subjected to **3a**-catalyzed hydrogenation. The secondary alcohols could be obtained in 84–97% *ee*s with quantitative conversion, indicating the high reactivity and enantioselectivity of the catalyst system. As shown in Table 4, the electronic and steric characteristics of substitu-

Table 4. Hydrogenation of various aryl ketones catalyzed by (*R*,*R*)-**3a**.[a]

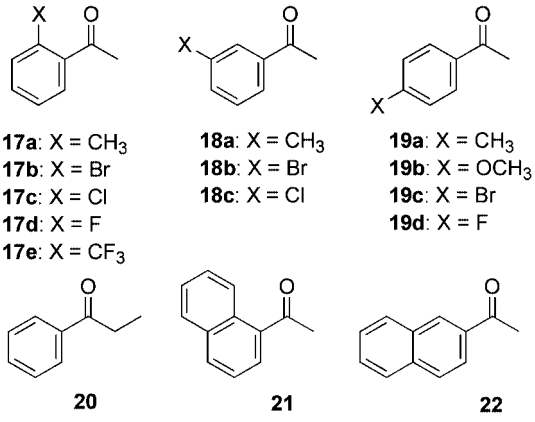

Entry	Aryl ketone	t [h]	*ee*[b]
1	**11**	4	91 (*S*)
2	**17a**[c]	5	97 (*S*)
3	**17b**	4	94 (*S*)
4	**17c**	5	90 (*S*)
5	**17d**	4	85 (*S*)
6	**17e**	4	91 (*S*)
7	**18a**	4	91 (*S*)
8	**18b**	4	87 (*S*)
9	**18c**	5	84 (*S*)
10	**19a**[c]	5	92 (*S*)
11	**19b**	6	89 (*S*)
12	**19c**	6	86 (*S*)
13	**19d**	5	87 (*S*)
14	**10**	4	92 (*S*)
15	**21**	5	95 (*S*)
16	**21**[c]	5	97 (*S*)
17	**22**	6	91 (*S*)

[a] Conditions: [**3a**] = 1.5 mM, [ketone] = 1.5 M (S/C = 1000), [KO*t*Bu] = 30 mM, $P(H_2)$ = 20 atm, t = 6 h, T = 25 °C. The conversion (>99%) was determined by ^{1}H NMR spectroscopy. [b] Determined by GC (Supelco BETA-DEX 120). The configurations of products were determined by $[\alpha]_D$. [c] *i*PrOH was used as solvent.

ents in the substrates had a dramatic influence on the enantioselectivity of the reaction. Sterically more demanding substituents on aromatic rings of ketones are obviously favorable for enantioselective control, while electron-withdrawing substituents generally have an adverse influence on product *ee*. The hydrogenations of 2-methylacetophenone (**17a**) and 1-acetonaphthone (**21**), for example, afforded the corresponding secondary alcohols with 97% *ee*s (Entries 2 and 16). Overall, the catalyst is superior to [$RuCl_2${BIPHEP}{(*S*,*S*)-DPEN}] (**2**) [7a] and comparable to the original Noyori catalyst [$RuCl_2${(*R*)-BINAP}{(*R*,*R*)-DPEN}] (**1**) in the hydrogenation of a variety of ketonic substrates.[2a]

Kinetics and Chiral Induction

In order to provide insight into the hydrogenation system, reaction profiles were collected for catalysts formed in situ [**13** + (*R*,*R*)-**14a**] and for preformed catalysts (**3a**) under the analogous conditions indicated in Figure 2. The hydrogenations were conducted in a glass autoclave fitted with a sampling needle connected to a stop valve, allowing for sample aliquots from the reaction mixture to be analyzed.

It was found that the substrate consumption as a function of time is sigmoidal in nature, due to the existence of an incubation period (Figure 2, a), which shows that preformed catalyst has a shorter incubation time and achieves its maximum reaction rate much more rapidly than the catalyst formed in situ. As shown in Figure 2 (b), the reaction profile with **3a** shows that the product (*S*)-**12** is generated with a constant *ee* value of 90% during the entire course of the reaction following the initial incubation period, which suggests that the active catalyst does not change during the catalysis under the reaction conditions and implies that the carbonyl moiety of the ligand in the catalyst is not reduced in the catalytic process.[16] Additionally, hydrogenation with the benzophenone-based bisphosphane ligand **9a** as substrate in the presence of complex **3a** under identical experimental conditions did not afford any hydrogenation product. Importantly, consumption of **11** in the system followed pseudo-first order kinetics after the incubation period, thanks to which the linearity of the expression $\ln[\mathbf{11}]_t = k_{obs}(t) + \ln[\mathbf{11}]_0$ ($[\mathbf{11}]_0 = [\mathbf{11}]$ at $t = 0$) allowed for determination of k_{obs} (Figure 2c). This observation is consistent with that found in Noyori's catalyst system.[4a] The hydrogenation was found to be twice as fast for preformed catalyst (**3a**) than for the in situ catalyst [**13** + (*R*,*R*)-**14a**].

As shown in the crystal structure of complex **3a** (Figure 1c), (*R*,*R*)-DPEN has induced an (*M*) conformation (right-handed) chirality for ligand **9a** in the complex. The ^1H and ^{31}P NMR of **3a**–**d** also each confirmed the presence of only one diastereomer for the complex in solution. The absolute configuration of the hydrogenation product obtained with this catalyst is (*S*), as described above. From the relationship between the absolute structures of Ru^{II} catalysts and the sense of asymmetric induction in the product reported by Noyori in BINAP-based catalysts[2] and by Mikami in BIPHEP-based catalysts,[7a] it can be concluded

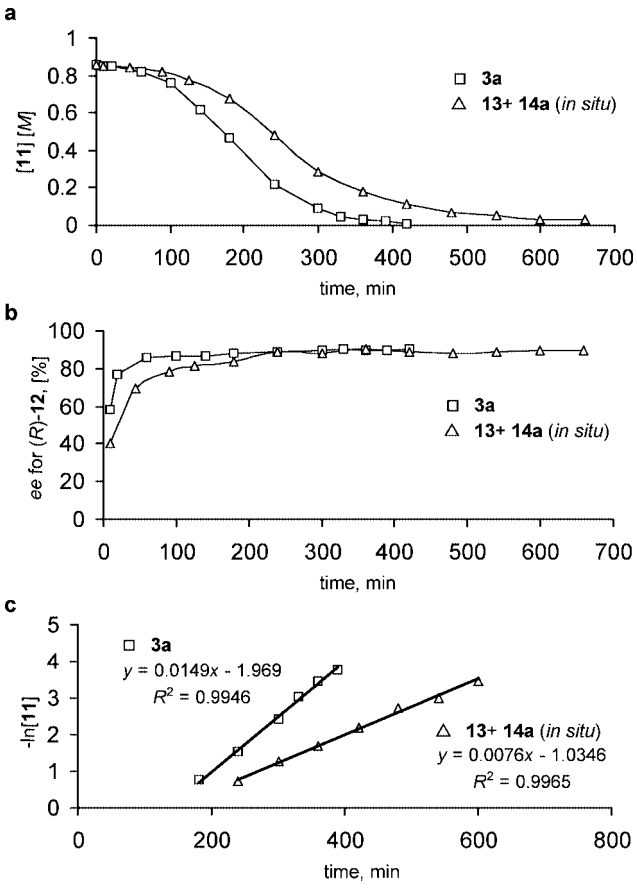

Figure 2. a) Reaction profiles for asymmetric hydrogenation of acetophenone (**11**) catalyzed by preformed **3a** and analogous catalyst generated in situ (**13** + **14a**). Conditions: [**3**] = 0.86 mM (or [**13**] = 0.86 mM + [**14a**] = 1.03 mM), [**11**] = 0.86 M, [KO*t*Bu] = 17.2 mM, $P(H_2)$ = 15 atm, T = 25 °C, ethanol solvent. b) Enantiomeric excess (*ee*) for product (*S*)-**12** in part a. c) Determination of rate constants (k_{obs}) for data in Part a. Only data points beyond the observed incubation period that resulted in linearity were used in calculation.

that the induced chirality for **9a** by (*R*,*R*)-DPEN (**14a**) in **3a** should be *pseudo*-(*R*), consistent with the structure observed in the solid-state investigation of **3a**. CD spectra of complexes **3a** generated with (*R*,*R*)-DPEN and (*S*,*S*)-DPEN show clear chiral signatures dependant on the chirality of the constituent 1,2-diamine, but distinct from those of the free 1,2-diamine enantiomers themselves. In contrast, the analogous complex with achiral ethylenediamine shows negligible absorbance (see Figure S2 in the Supporting Information).

In conjunction with the structure of the precatalyst **3a** and the observed sense of asymmetric induction, the formation of (*S*) product is believed to be the result of the λ-configuration of (*R*,*R*)-1,2-diamine around the Ru^{II} center[4a] and the consequently induced chirality of the constituent bisphosphane ligand. A proposed mode of asymmetric induction for the catalyst system, based on the molecular structure of the catalyst precursor **3a** (Figure 1c), is thus depicted in Figure 3. Here it is assumed that the (C=O) Ru^{II} interaction itself persists during the hydrogenation step, keeping the configuration of the potentially flexible **9**

(and **10**) "locked". This is reasonable in view of the higher observed *ee* values in relation to the BINAP analogue **1**. A comparison of the two transition structures TS-*Re* and TS-*Si* shows that the bulkier phenyl ring in the substrate should be suitable for orientation in the less hindered space and should form a preferential transition state (TS-*Re*) to provide the hydrogenation product in the (*S*) configuration, which is consistent with the observed hydrogenation outcome.

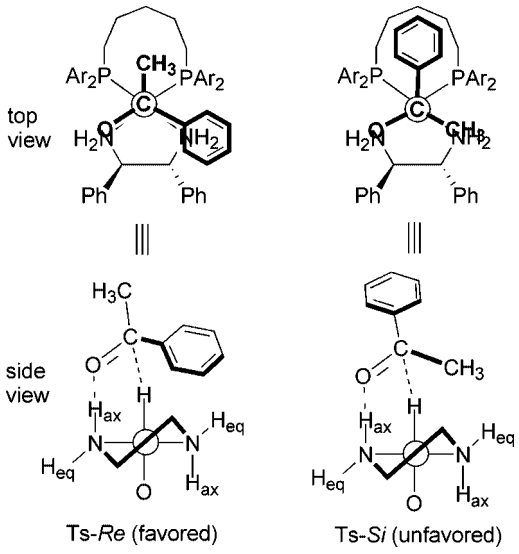

Figure 3. Schematic representation of asymmetric induction mode in asymmetric hydrogenation of acetophenone with **3**.

Conclusions

In summary, we have developed a new type of Ru^{II} catalysts (**3**) composed of benzophenone-based achiral bisphosphane ligands and enantiopure 1,2-diamines for asymmetric hydrogenation of aryl ketones. The catalysts exhibited excellent enantioselectivities (up to 97% *ee*) and activities (up to S/C = 10,000) in the hydrogenation of a variety of aromatic ketones. Complete chirality induction from the enantiopure 1,2-diamine to the flexible benzophenone-based achiral bisphosphane ligand was demonstrated. The coordination of C=O to the cationic Ru^{II} center is believed to be the key feature in providing the thermodynamic and kinetic bias for single diastereomer formation. Such a strategy greatly improves the potential for the design of enantiopure catalysts incorporating chirally flexible chiral ligands and enantiopure 1,2-diamines. The results obtained in this work should stimulate further research on the development of practical catalysts for enantioselective hydrogenation of ketones in the presence of achiral bisphosphane ligands.

Experimental Section

General Methods: All manipulations involving air- and moisture-sensitive compounds were carried out by use of standard Schlenk technique under argon or in a Braun Labmaster glove box. Unless otherwise noted, NMR spectra were recorded in $CDCl_3$ on a Varian Mercury 300 (^{1}H 300 MHz; ^{13}C 75 MHz. ^{19}F NMR 282 MHz. ^{31}P NMR 121 MHz) spectrometer at room temperature. Chemical shifts are reported in ppm with TMS (δ =0 ppm) for ^{1}H and $CDCl_3$ (δ =77.0 ppm) for ^{13}C as internal standards. ^{31}P NMR spectra were recorded with 85% H_3PO_4 as an external reference. The FT-IR spectra were measured with a Rio-Rad FTS-185 spectrometer in KBr pellets. EI-MS (70 eV) and ESI-MS spectra were obtained with HP5989A and Mariner LC-TOF spectrometers, respectively. MALDI-TOF mass spectra were measured with a MATRIX VOYAGR-DE STR fitted with a 337 nm nitrogen laser, with α-cyano-4-hydroxycinnamic acid (α-CHCA) as the matrix and sodium trifluoroacetate as the ionization agent. HRMS were determined on an IonSpect 4.7 TESLA FTMS instrument. Elemental analyses were performed with an Elemental VARIO EL apparatus. GC analyses were measured with an Agilent 6890N system. Optical rotations were measured with a Perkin–Elmer 341 automatic polarimeter, and CD spectra were taken with a JASCO 810 spectropolarimeter. The X-ray diffraction intensity data were collected with a Bruker CCD Smart APEX diffractometer at 20 °C. Dichloromethane, chloroform, and tetrachloromethane were freshly distilled from calcium hydride, THF and toluene from sodium benzophenone ketyl, and ethyl acetate from P_2O_5. 2-Methoxybenzaldehyde and 2-methoxyphenyl bromide were purchased from Acros and were used without further purification.

Ligand Synthesis: Compounds **4b**–**c**,[17] **5a**,[10] **6a**,[11] **7a**–**b**,[12] and 4-*tert*-butyl-2-methoxybenzaldehyde and 5-*tert*-butyl-2-methoxybenzaldehyde[18] were prepared by the corresponding literature procedures.

Bis(5-*tert*-butyl-2-methoxyphenyl)methanol (5b): Treatment of **4b** with magnesium powder and 5-*tert*-butyl-2-methoxybenzaldehyde in anhydrous THF by a procedure similar to that used for preparation of **5a**[10] afforded **5b** as a white solid in 73% yield. M.p. 85–86 °C [ref.[10b] 84–86 °C]. ^{1}H NMR (300 MHz, $CDCl_3$): δ = 7.34 (d, J = 2.4 Hz, 2 H), 7.22 (dd, J = 8.7, 2.4 Hz, 2 H), 6.79 (d, J = 8.7 Hz, 2 H), 6.26 (d, J = 6.0 Hz, 1 H), 3.79 (s, 6 H), 1.27 (s, 18 H) ppm. ^{13}C NMR (75 MHz, $CDCl_3$): δ = 154.5, 142.8, 130.1, 125.3, 124.6, 109.8, 68.9, 55.2, 34.0, 31.4 ppm.

Bis(4-*tert*-butyl-2-methoxyphenyl)methanol (5c): Treatment of **4c** with magnesium powder and 4-*tert*-butyl-2-methoxybenzaldehyde in anhydrous THF by a procedure similar to that used for preparation of **5a**[10] afforded **5c** as a white solid in 84% yield. M.p. 91–92 °C [ref.[10a] 89–90 °C]. ^{1}H NMR (300 MHz, $CDCl_3$): δ = 7.13 (d, J = 7.8 Hz, 2 H), 6.94 (dd, J = 7.8, 1.8 Hz, 2 H), 6.91 (d, J = 1.8 Hz, 2 H), 6.29 (d, J = 5.1 Hz, 1 H), 3.82 (s, 6 H), 3.63 (d, J = 5.1 Hz, 1 H), 1.32 (s, 18 H) ppm.

Bis(5-*tert*-butyl-2-methoxyphenyl)methanone (6b): Oxidation of **5b** with $K_2Cr_2O_7$ in DMF at 100 °C for 8 hours by a procedure similar to that used for preparation of **6a**[11] afforded **6b** as a yellow solid in 88% yield. M.p. 88–90 °C [ref.[11b] 90–92 °C]. ^{1}H NMR (300 MHz, $CDCl_3$): δ = 7.52 (d, J = 2.7 Hz, 2 H), 7.44 (dd, J = 8.4, 2.7 Hz, 2 H), 6.84 (d, J = 8.4 Hz, 2 H), 3.65 (s, 6 H), 1.24 (s, 18 H) ppm. ^{13}C NMR (75 MHz, $CDCl_3$): δ = 195.8, 156.2, 142.8, 129.4, 129.2, 127.4, 111.2, 55.8, 34.0, 31.3 ppm.

Bis(4-*tert*-butyl-2-methoxyphenyl)methanone (6c): Oxidation of **5c** with $K_2Cr_2O_7$ in DMF at 100 °C for 10 hours by a procedure similar to that used for preparation of **6a**[11] afforded **6c** as a yellow solid in 91% yield. M.p. 90–91 °C. ^{1}H NMR (300 MHz, $CDCl_3$): δ = 7.42 (d, J = 8.1 Hz, 2 H), 7.00 (dd, J = 8.1, 1.8 Hz, 2 H), 6.92 (d, J = 1.8 Hz, 2 H), 3.71 (s, 6 H), 1.33 (s, 18 H) ppm. ^{13}C NMR (75 MHz, $CDCl_3$): δ = 194.9, 158.2, 156.4, 130.4, 127.5, 117.3, 108.9, 55.8, 35.2, 31.1 ppm. FT-IR (KBr pellet): $\tilde{\nu}$ = 2963, 2868,

1641, 1608, 1410, 1309, 1236, 1038, 941, 822, 686, 597 cm^{-1}. EI-MS (70 ev): *m/z* 354 $[M]^+$ (40.4), 337 (47.2), 323 (36.9), 297 (59.3), 281 (46.2), 191 (100), 177 (73.9), 57 (89.6). Elemental analysis (%) calcd. for $C_{23}H_{30}O_3$ (354.22): C 77.93, H 8.53; found C 77.74, H 8.55.

Bis(5-*tert*-butyl-2-hydroxyphenyl)methanone (7b): Demethylation of **6b** with BBr_3 in dichloromethane and subsequent hydrolysis, by a procedure similar to that used for preparation of **7a**,[12] afforded **7b** as a yellow solid in 92% yield. M.p. 102–103 °C [ref.[11b] 104–106 °C]. ^1H NMR (300 MHz, $CDCl_3$): δ = 10.50 (s, 2 H), 7.62–7.58 (m, 4 H), 7.05 (d, *J* = 9.0 Hz, 2 H), 1.31 (s, 18 H) ppm. ^{13}C NMR (75 MHz, $CDCl_3$): δ = 202.8, 159.5, 141.4, 133.4, 129.1, 119.3, 118.1, 34.2, 31.3 ppm.

Bis(4-*tert*-butyl-2-hydroxyphenyl)methanone (7c): Demethylation of **6c** with BBr_3 in dichloromethane and subsequent hydrolysis, by a procedure similar to that used for preparation of **7a**,[12] afforded **7c** as a yellow solid in 90% yield. M.p. 135–136 °C. ^1H NMR (300 MHz, $CDCl_3$): δ = 10.80 (s, 2 H), 7.59 (d, *J* = 8.7 Hz, 2 H), 7.09 (d, *J* = 1.8 Hz, 2 H), 6.95 (dd, *J* = 8.7, 1.8 Hz, 2 H), 1.32 (s, 18 H) ppm. ^{13}C NMR (75 MHz, $CDCl_3$): δ = 201.1, 161.8, 160.3, 132.7, 117.3, 116.4, 115.2, 35.3, 30.8 ppm. FT-IR (KBr pellet): $\tilde{\nu}$ = 3243, 2958, 2866, 1623, 1581, 1500, 1350, 1193, 942, 880, 794, 693, 470 cm^{-1}. EI-MS (70 ev): *m/z* 326 $[M]^+$ (28.7), 325 (14.5), 310 (17.1), 309 (70.2), 269 (38.9), 177 (100), 176 (14.4), 134 (20.7). Elemental analysis (%) calcd. for $C_{21}H_{26}O_3$ (326.19): C 77.27, H 8.03; found C 77.57, H 7.87.

Bis(2-trifluoromethylsulfonyloxyphenyl)methanone (8a): Trifluoromethanesulfonic anhydride (6.0 mL, 34.7 mmol) was added dropwise at –78 °C over a 30 minute period to a stirred solution of **7a** (1.8 g, 8.4 mmol) and Et_3N (5 mL) in anhydrous dichloromethane (50 mL). The reaction mixture was allowed to warm to room temperature and stirred overnight. After removal of the solvent in vacuo, the residue was diluted with EtOAc (30 mL) and was then washed with aqueous HCl (5%), saturated $NaHCO_3$, and brine (once each). The organic layer was dried with Na_2SO_4 and concentrated under reduced pressure. The residue was purified by silica gel column chromatography with hexane/EtOAc (5:1) as eluent to give compound **8a** as a yellowish solid (3.6 g, 90% yield). M.p. 55–57 °C. ^1H NMR (300 MHz, $CDCl_3$): δ = 7.74–7.69 (m, 4 H), 7.54 (t, *J* = 8.1 Hz, 2 H), 7.42 (d, *J* = 8.1 Hz, 2 H) ppm. ^{13}C NMR (75 MHz, $CDCl_3$): δ = 189.1, 147.2, 134.2, 132.4, 131.5, 128.4, 122.4, 120.5, 116.3 ppm. ^{19}F NMR (282 MHz, $CDCl_3$): δ = –73.5 ppm. FT-IR (KBr pellet): $\tilde{\nu}$ = 3084, 1685, 1610, 1488, 1421, 1305, 1214, 1137, 1108, 1082, 948, 868, 767, 685, 603, 526 cm^{-1}. EI-MS (70 ev) *m/z*: 478 $[M]^+$ (56.6), 329 (47.5), 281 (17.8), 265 (70.7), 253 (100), 212 (65.0), 120 (53.4), 69 (55.1). HRMS (MALDI) *m/z* calcd. for $C_{15}H_8F_6O_7S_2$: 477.9616; found 477.9615.

Compounds **8b** and **8c** were synthesized by a procedure similar to that used for **8a**.

Bis(5-*tert*-butyl-2-trifluoromethylsulfonyloxyphenyl)methanone (8b): Yield 89%. M.p. 98–101 °C. ^1H NMR (300 MHz, $CDCl_3$): δ = 7.71 (d, *J* = 2.1 Hz, 2 H), 7.66 (dd, *J* = 8.7, 2.1 Hz, 2 H), 7.28 (d, *J* = 8.7 Hz, 2 H), 1.34 (s, 18 H) ppm. ^{13}C NMR (75 MHz, $CDCl_3$): δ = 189.9, 151.9, 144.8, 131.1, 131.0, 129.7, 121.7, 120.5, 116.3, 34.9, 31.0 ppm. ^{19}F NMR (282 MHz, $CDCl_3$): δ = –73.6 ppm. FT-IR (KBr pellet): $\tilde{\nu}$ = 2972, 2877, 1680, 1490, 1421, 1250, 1221, 1139, 881, 618, 586 cm^{-1}. ESI-MS: *m/z*: 591 $[M+H]^+$. Elemental analysis (%) calcd. for $C_{23}H_{24}F_6O_7S_2$ (590.09): C 46.78, H 4.10; found C 46.68, H 4.42.

Bis(4-*tert*-butyl-2-trifluoromethylsulfonyloxyphenyl)methanone (8c): Yield 94%. M.p. 105–107 °C. ^1H NMR (300 MHz, $CDCl_3$): δ = 7.60 (d, *J* = 8.1 Hz, 2 H), 7.47 (d, *J* = 8.1 Hz, 2 H), 7.26 (s, 2 H), 1.36 (s, 18 H) ppm. ^{13}C NMR (75 MHz, $CDCl_3$): δ = 188.8, 158.9, 147.2, 132.2, 128.7, 125.1, 120.6, 119.6, 116.3, 35.4, 30.7 ppm. ^{19}F NMR (282 MHz, $CDCl_3$): δ = –73.6 ppm. FT-IR (KBr pellet): $\tilde{\nu}$ = 2969, 2876, 1680, 1617, 1426, 1221, 1136, 969, 892, 844, 790, 603, 515 cm^{-1}. ESI-MS: *m/z*: 613 $[M+Na]^+$. Elemental analysis (%) calcd. for $C_{23}H_{24}F_6O_7S_2$ (590.09): C 46.78, H 4.10; found C 46.80, H 4.16.

Bis(2-diphenylphosphanylphenyl)methanone (9a): Degassed DMF (6 mL), Ph_2PH (700 mg, 3.76 mmol), and diisopropylethylamine (1.5 mL) were added to a mixture of **8a** (600 mg, 1.26 mmol) and $NiCl_2$(dppp) (66 mg, 0.126 mmol) in a vial. The resulting mixture was heated with stirring at 100 °C for 20 min, after which another aliquot of Ph_2PH (200 mg) was added, and was then stirred at the same temperature for 10 hours. After completion of the reaction, the mixture was cooled to room temperature and the reaction was quenched with HCl (1 N). The resultant mixture was extracted with ethyl acetate, and the organic phase was washed with brine, dried with anhydrous Na_2SO_4, and concentrated in vacuo. The residue was purified by silica gel column chromatography with hexane/EtOAc (10:1) as eluent to afford **9a** as a yellow powder (690 mg, 45% yield). M.p. 135–138 °C. ^1H NMR (300 MHz, $CDCl_3$): δ = 7.32–7.22 (m, 28 H) ppm. ^{13}C NMR (75 MHz, $CDCl_3$): δ = 198.0, 143.6, 143.3 139.3, 139.0, 137.7, 137.5, 134.6, 134.0, 133.8, 133.7, 130.8, 128.3, 128.2, 127.9 ppm. ^{31}P NMR (121 MHz, $CDCl_3$): δ = –7.3 ppm. FT-IR (KBr pellet): $\tilde{\nu}$ = 3049, 1652, 1608, 1582, 1479, 1296, 1275, 1241, 1125, 929, 746, 693, 498 cm^{-1}. EI-MS (70ev) *m/z*: 550 $[M]^+$ (63.0), 473 (58.0), 349 (73.8), 270 (100), 201 (65.5), 183 (74.5), 77 (29.5). Elemental analysis (%) calcd. for $C_{37}H_{28}OP_2$ (550.16): C 80.72, H 5.12; found C 80.60, H 5.13.

Single-Crystal X-ray Analysis of 9a: Single crystals of **9a** were obtained by recrystallization from CH_2Cl_2/hexane (1:3). The X-ray diffraction intensity data were collected with a Bruker CCD Smart diffractometer at 20 °C with use of Mo-K_α radiation (λ = 0.71073 Å). Crystallographic data: formula $C_{37}H_{28}OP_2$, The structure was solved by direct method by use of the SHELXTL-97 software package with monoclinic space group *Pbca*, with unit cell dimensions, Z = 8, ρ_{calc} = 1.263 g·cm^{-3}. The integration of the data yielded a total of 32952 reflections, of which 6607 were independent and 3415 were greater than 2σ(*I*). The structure was refined to R_1 = 0.0462, wR_2 = 0.1012, and Goodness of Fit = 0.854.

Compounds **9b** and **9c** were synthesized by a procedure similar to that used for **9a**.

Bis[5-*tert*-butyl-2-(diphenylphosphanyl)phenyl]methanone (9b): Yield 38%. M.p. 197–198 °C. ^1H NMR (300 MHz, $CDCl_3$): δ = 8.33 (d, *J* = 2.4 Hz, 2 H), 7.79 (dd, *J* = 8.7, 2.4 Hz, 2 H), 7.43–7.36 (m, 4 H), 7.29–7.23 (m, 16 H), 7.03 (dd, *J* = 8.1, 3.6 Hz, 2 H), 1.19 (s, 18 H) ppm. ^{13}C NMR (75 MHz, $CDCl_3$): δ = 198.7, 154.3, 150.8, 146.7, 138.2, 138.0, 134.3, 133.7, 312.5, 128.1, 127.90, 122.4, 121.0, 117.5, 34.7, 34.5, 31.3, 31.1 ppm. ^{31}P NMR (121 MHz, $CDCl_3$): δ = –7.8 ppm. FT-IR (KBr pellet): $\tilde{\nu}$ = 2962, 2868, 1660, 1471, 1434, 1239, 975, 741, 695, 502 cm^{-1}. ESI-MS: *m/z*: 663 $[M+H]^+$. Elemental analysis (%) calcd. for $C_{45}H_{44}OP_2$ (662.29): C 81.55, H 6.69; found C 81.39, H 6.45.

Bis[4-*tert*-butyl-2-(diphenylphosphanyl)phenyl]methanone (9c): Yield 50%. M.p. 169–172 °C. ^1H NMR (300 MHz, $CDCl_3$): δ = 7.29–7.20 (m, 22 H), 7.15–7.08 (m, 4 H), 1.07 (s, 18 H) ppm. ^{13}C NMR (75 MHz, $CDCl_3$): δ = 197.7, 153.5, 141.19, 140.8, 138.6, 138.3, 138.1, 138.0, 133.9, 133.8, 133.6, 132.3, 130.8, 128.2, 128.1, 128.0, 124.5, 34.8, 30.8 ppm. ^{31}P NMR (121 MHz, $CDCl_3$): δ = –6.3 ppm. FT-IR (KBr pellet): $\tilde{\nu}$ = 2962, 2866, 1653, 1585, 1433, 1307, 1261, 1118, 936, 745, 694, 500 cm^{-1}. MS (MALDI-TOF) *m/z*: 663

$[M+H]^+$. Elemental analysis (%) calcd. for $C_{45}H_{44}OP_2$ (662.29): C 81.55, H 6.69; found C 81.50, H 6.52.

Bis{2-[bis(3,5-dimethylphenyl)phosphanyl]phenyl}methanone (10): Compound **10** was prepared by a procedure similar to that used for **9a**, with 1:1-bis(3,5-dimethylphenyl)phosphane/borane complex as the phosphanylation reagent. Yield 25%. M.p. 186–188 °C. ^{1}H NMR (300 MHz, $CDCl_3$): δ = 7.16–7.06 (m, 6 H), 6.93–6.83 (m, 10 H), 6.74 (d, J = 6.0 Hz, 4 H), 2.25 (s, 12 H, CH_3), 2.15 (s, 12 H, CH_3) ppm. ^{13}C NMR (75 MHz, $CDCl_3$): δ = 199.6, 147.3, 137.7, 137.6, 137.1, 135.8, 134.5, 134.1, 131.8, 131.6, 131.4, 131.3, 131.1, 130.3, 130.1, 130.0, 128.4, 127.5, 127.4, 127.2, 21.1 ppm. ^{31}P NMR (121 MHz, $CDCl_3$): δ = –16.9 ppm. FT-IR (KBr pellet): $\tilde{\nu}$ = 2912, 2855, 1663, 1582, 1438, 1299, 1126, 1005, 928, 846, 758, 692 cm^{-1}. MS(MALDI) *m*/*z*: 663 $[M+H]^+$. HRMS (MALDI) *m*/*z* calcd. for $C_{45}H_{44}OP_2$ $[M+H]^+$ 663.2946; found 663.2928.

Typical Procedure for the Preparation of Precatalyst *trans*-RuCl$_2$[9a]](*R*,*R*)-14a] (3a): Anhydrous DMF (4 mL) was added at room temperature under argon to a mixture of ligand **9a** (200 mg, 0.363 mmol) and $[RuCl_2(C_6H_6)]_2$ (90 mg, 0.181 mmol) in a Schlenk tube. After being stirred at 100 °C for 25 minutes, the mixture was cooled to 50 °C and the solvent was removed in vacuo. Anhydrous CH_2Cl_2 (3 mL) and (*R*,*R*)-DPEN (93 mg, 0.436 mmol) were added to the residue and the solution was stirred at room temp. for 6 hours. Reduction of the volume to ca 1.0 mL and addition of hexane (6 mL) yielded a yellow precipitate. The supernatant was removed by filtration and the resulting powder was dried in vacuo to give a 82% yield (278 mg) of **3a**, which was used for hydrogenation without further purification. M.p. 170 °C (dec.). ^{1}H NMR (300 MHz, $CDCl_3$): δ = 8.15 (d, J = 7.5 Hz, 1 H), 8.06 (d, J = 7.5 Hz, 1 H), 7.81 (t, J = 7.8 Hz, 1 H), 7.69 (t, J = 7.8 Hz, 1 H), 7.53 (t, J = 7.5 Hz, 1 H), 7.44 (t, J = 7.5 Hz, 1 H), 7.33–7.27 (m, 10 H), 7.23–7.09 (m, 14 H), 7.05–6.99 (m, 6 H), 6.95–6.90 (m, 2 H), 4.67 (m, 1 H), 4.53 (m, 1 H), 3.52 (br., 1 H), 3.21 (br., 1 H), 3.09–3.01 (m, 2 H) ppm. ^{31}P NMR (121 MHz, $CDCl_3$): δ = 47.7 (d, J = 22.8 Hz), 47.2 (d, J = 23.6 Hz) ppm. FT-IR (KBr pellet): $\tilde{\nu}$ = 3314, 3207, 3057, 1665, 1435, 1387, 1096, 1029, 724, 699, 528 cm^{-1}. MS (MALDI) *m*/*z*: 899 $[M-Cl]^+$. Elemental analysis (%) calcd. for $C_{51}H_{44}Cl_2N_2OP_2Ru\cdot 2H_2O$ (970.16): C 63.09, H 4.98, N 2.89; found C 62.76, H 5.14, N 2.93.

X-ray Single Crystallographic Analysis of 3a: Single crystals of **3a** were obtained by recrystallization from CH_2Cl_2/hexane (1:2). The X-ray diffraction intensity data were collected with a Bruker CCD Smart diffractometer at 20 °C with use of Mo-K_α radiation (λ = 0.71073 Å). Crystallographic data: formula $C_{106}H_{106}Cl_8N_4O_{10}P_4Ru_2$. The structure was solved by direct methods with use of the SHELXTL-97 software package using monoclinic space group C_2, with unit cell dimensions, Z = 4, ρ_{calc} = 1.308 g·cm^{-3}. The integration of the data yielded a total of 33023 reflections, of which 22198 were independent and 16076 were greater than 2σ(I). The structure was refined to R_1 = 0.0795, wR_2 = 0.2073, and Goodness of Fit = 1.067. Absolute structural parameter was –0.03(4).

CCDC-602529 and -602530 contain the supplementary crystallographic data for this paper. These data can be obtained free of charge from The Cambridge Crystallographic Data Centre via www.ccdc.cam.ac.uk/data_request/cif.

Complexes **3b**, **3c** and **3d** were synthesized by a procedure similar to that used for **3a**.

***trans*-RuCl$_2$[9b]](*R*,*R*)-14a] (3b):** Yield 82%. M.p. 218 °C (dec.). ^{1}H NMR (300 MHz, $CDCl_3$): δ = 8.00 (s, 2 H), 7.57 (d, J = 8.1 Hz, 2 H), 7.50 (d, J = 8.1 Hz, 2 H), 7.46–7.35 (m, 12 H), 7.23–7.16 (m, 10 H), 7.08–6.96 (m, 8 H), 4.59–4.50 (m, 2 H), 3.35–3.31 (m, 1 H), 3.19 (br., 1 H), 3.09 (br., 1 H), 2.76–2.73 (m, 1 H), 1.45 (s, 9 H), 1.42 (s, 9 H) ppm. ^{31}P NMR (121 MHz, $CDCl_3$): δ = 46.4 (d, J = 23.5 Hz), 53.2 (d, J = 23.0 Hz) ppm. FT-IR (KBr pellet): $\tilde{\nu}$ = 3312, 3192, 2960, 1667, 1481, 1435, 1150, 1028, 738, 698 cm^{-1}. MS (MALDI) *m*/*z*: 1011 $[M-Cl]^+$.

***trans*-RuCl$_2$[9c]](*R*,*R*)-14a] (3c):** Yield 80%. M.p. 202 °C (dec.). ^{1}H NMR (300 MHz, $CDCl_3$): δ = 8.07–7.98 (m, 2 H), 7.78 (d, J = 7.8 Hz, 1 H), 7.70 (d, J = 7.8 Hz, 1 H), 7.32–7.27 (m, 14 H), 7.23–7.19 (m, 10 H), 7.05–6.92 (m, 8 H), 4.58–4.53 (m, 1 H), 4.44–4.41 (m, 1 H), 4.30 (br., 1 H), 3.08–3.01 (m, 2 H), 2.74 (br., 1 H), 1.24 (s, 9 H), 1.20 (s, 9 H) ppm. ^{31}P NMR (121 MHz, $CDCl_3$): δ = 47.8 (d, J = 23.6 Hz), 47.4 (d, J = 23.4 Hz) ppm. FT-IR (KBr pellet): $\tilde{\nu}$ = 3315, 3259, 2960, 2868, 1669, 1483, 1388, 1246, 1094, 1029, 698 cm^{-1}. MS (MALDI) *m*/*z*: 1011 $[M-Cl]^+$.

***trans*-RuCl$_2$[10]](*R*,*R*)-14a] (3d):** Yield 84%. M.p. 165–168 °C. ^{31}P NMR (121 MHz, $CDCl_3$): δ = 54.1 (d, J = 37.2 Hz), 53.2 (d, J = 36.4 Hz) ppm. FT-IR (KBr pellet): $\tilde{\nu}$ = 3059, 3030, 2918, 1670, 1454, 1383, 1128, 1028, 698, 566 cm^{-1}. MS (MALDI) *m*/*z*: 1011 $[M-Cl]^+$.

General Procedure for Ru-Catalyzed Asymmetric Hydrogenation of Ketones (Method A): EtOH (2.0 mL) was introduced under argon into a test tube containing the precatalyst (0.003 mmol), KO*t*Bu (6.7 mg, 0.06 mmol), and a stirring bar. Aromatic ketone (3.0 mmol) was added after the mixture had been stirred for 10 minutes. The resulting mixture was placed in an autoclave under argon. After purging with hydrogen (5 times), the final H_2 pressure was adjusted to 300 psi (20 atm). After the desired reaction time (typically 6 hours) at room temperature, the reaction was stopped by releasing the hydrogen gas. The solvent was removed and the degree of conversion was determined by ^{1}H NMR analysis. The residue was filtered through a short silica gel column (5 cm, hexane/EtOAc 2:1), and the enantiomeric excess of the product was determined by chiral GC (Supelco BETA™ 120 column).

General Procedure for Ru-Catalyzed Asymmetric Hydrogenation of Ketones (Method B): EtOH (2.0 mL) was introduced under argon into a test tube containing the complex RuCl$_2$[**9a**](dmf)$_2$ (**13**) (2.2 mg, 0.003 mmol), KO*t*Bu (6.7 mg, 0.06 mmol), diamine (0.0036 mol), and a stirring bar. The aromatic ketone (3.0 mmol) was added after the mixture had been stirred for 20 minutes. The resulting mixture was placed in an autoclave under argon. After purging with hydrogen (5 times), the final H_2 pressure was adjusted to 300 psi (20 atm). After a reaction time of 10 hours, the reaction was stopped by releasing the hydrogen gas. The solvent was removed and the degree of conversion was determined by ^{1}H NMR analysis. The residue was filtered through a short silica gel column (5 cm, hexane/EtOAc 2:1), and the enantiomeric excess of the product was determined by chiral GC (Supelco BETA™ 120 column).

Reaction Profile Measurement and Determination of k_{obs} for *trans*-RuCl$_2$[9a]](*R*,*R*)-14a] (3a) Catalyzed Hydrogenation of Acetophenone: Hydrogenations were conducted in a glass autoclave fitted with a sampling needle attached to a three-way stop valve. This setup allowed for sample aliquots to be taken from the active reaction mixture for analysis (^{1}H NMR, GC). An accurately measured mass of **3a** [or **13** and (*R*,*R*)-**14a**], together with solid KO*t*C$_4$H$_9$, were added to a predried glass autoclave containing a magnetic stirring bar, and the system was then maintained under vacuum for 5 minutes prior to purging with argon. A degassed ethanol solution of substrate **11** (0.86 M) was then added to the autoclave under argon. Hydrogen was introduced at 5 atmospheres pressure, with several quick release-fill cycles before being set to the desired pressure. Stirring and timing (t = 0) were immediately commenced. Reaction samples were obtained at specified time intervals for analy-

sis. Conditions: [**3a**] = 0.86 mM (or [**13**] = 0.86 mM + [**14a**] = 1.03 mM), [**11**] = 0.86 M, [KO*t*Bu] = 17.2 mM, $P(H_2)$ = 15 atm, T = 25 °C, ethanol solvent. Determination of rate constants (k_{obs}) was calculated from reaction profile data. Only data points beyond the observed incubation period that resulted in linearity were used in calculation. The values of k_{obs} were determined from the gradient of: $\ln[\mathbf{11}]_t = k_{obs}(t) + \ln[\mathbf{11}]_0$ ($[\mathbf{11}]_0 = [\mathbf{11}]$ at $t = 0$).

Supporting Information (see footnote on the first page of this article): Mass spectra of **3a**–**d**, CD spectra of **3a**, Table S1 (conversion/time relationship), ^{1}H NMR and GC analysis of hydrogenation products.

Acknowledgments

Financial support from the National Natural Science Foundation of China, the Chinese Academy of Sciences, the Major Basic Research Development Program of China (Grant no. G2000077506), and the Committee of Science and Technology of Shanghai Municipality is gratefully acknowledged.

[1] a) T. Ohkuma, R. Noyori, in *Comprehensive Asymmetric Catalysis*, vol. 1 (Eds.: E. N. Jacobsen, A. Pfaltz, H. Yamamoto), Springer, Berlin, **1999**, chapter 6.1; b) T. Ohkuma, M. Kitamura, R. Noyori, in *Catalytic Asymmetric Synthesis* (Ed.: I. Ojima), Wiley-VCH, New York, **2000**, chapter 1; c) T. Ohkuma, R. Noyori, in *Transition Metals for Organic Synthesis: Building Blocks and Fine Chemicals*, vol. 2 (Eds.: M. Beller, C. Bolm) Wiley-VCH, Weinheim, **1998**, pp. 25–69; for comprehensive reviews, see: d) R. Noyori, T. Ohkuma, *Angew. Chem.* **2001**, *113*, 40–75; *Angew. Chem. Int. Ed.* **2001**, *40*, 40–73; e) W. Tang, X. Zhang, *Chem. Rev.* **2003**, *103*, 3029–3070; f) H.-U. Blaser, C. Malan, B. Pugin, F. Spindler, H. Steiner, M. Studer, *Adv. Synth. Catal.* **2003**, *345*, 103–151.

[2] For leading references, see: a) T. Ohkuma, H. Ooka, T. Ikariya, R. Noyori, *J. Am. Chem. Soc.* **1995**, *117*, 10417–10418; b) T. Ohkuma, H. Ooka, S. Hashiguchi, T. Ikariya, R. Noyori, *J. Am. Chem. Soc.* **1995**, *117*, 2675–2676; c) H. Doucet, T. Ohkuma, K. Murata, T. Yokozawa, M. Kozawa, E. Katayama, A. F. England, T. Ikariya, R. Noyori, *Angew. Chem.* **1998**, *110*, 1792–1796; *Angew. Chem. Int. Ed.* **1998**, *37*, 1703–1707; d) T. Ohkuma, M. Koizumi, H. Doucet, T. Pham, M. Kozawa, K. Murata, E. Katayama, T. Yokozawa, T. Ikariya, R. Noyori, *J. Am. Chem. Soc.* **1998**, *120*, 13529–13530; e) T. Ohkuma, D. Ishii, H. Takeno, R. Noyori, *J. Am. Chem. Soc.* **2000**, *122*, 6510–6511; f) T. Ohkuma, M. Koizumi, K. Muñiz, G. Hilt, C. Kabuto, R. Noyori, *J. Am. Chem. Soc.* **2002**, *124*, 6508–6509.

[3] For examples of catalysts analogous to Noyori's, see: a) P. Cao, X. Zhang, *J. Org. Chem.* **1999**, *64*, 2127–2129; b) M. J. Burk, W. Hems, D. Herzberg, C. Malan, A. Zanotti-Gerosa, *Org. Lett.* **2000**, *2*, 4173–4174; c) J. H. Xie, L. X. Wang, Y. Fu, S. F. Zhu, B. M. Fan, H. F. Duan, Q. L. Zhou, *J. Am. Chem. Soc.* **2003**, *125*, 4404–4405; d) J. Wu, J. X. Ji, R. Guo, C.-H. Yeung, A. S. C. Chan, *Chem. Eur. J.* **2003**, *9*, 2963–2968; e) J. P. Henschke, A. Zanotti-Gerosa, P. Moran, P. Harrison, B. Mullen, G. Casy, I. C. Lennon, *Tetrahedron Lett.* **2003**, *44*, 4379–4383; f) A. Hu, H. L. Ngo, W. Lin, *Org. Lett.* **2004**, *6*, 2937–2940; g) R. Guo, R. H. Morris, D. Song, *J. Am. Chem. Soc.* **2005**, *127*, 516–517; h) D. G. Genov, D. J. Ager, *Angew. Chem.* **2004**, *116*, 2876–2879; *Angew. Chem. Int. Ed.* **2004**, *43*, 2816–2819.

[4] For mechanism of asymmetric hydrogenation of ketones catalyzed by [$RuCl_2${BINAP}{diamine}] complexes, see: a) C. A. Sandoval, T. Ohkuma, K. Kuniz, R. Noyori, *J. Am. Chem. Soc.* **2003**, *125*, 13490–13503; b) R. Hartmann, P. Chan, *Angew. Chem.* **2001**, *113*, 3693–3697; *Angew. Chem. Int. Ed.* **2001**, *40*, 3581–3585; c) K. Abdur-Rashid, M. Faatz, A. J. Lough, R. H. Morris, *J. Am. Chem. Soc.* **2001**, *123*, 7473–7474.

[5] For comprehensive reviews on asymmetric activation, see: a) K. Mikami, M. Terada, T. Korenaga, Y. Matsumoto, M. Ueki, R. Angelaud, *Angew. Chem.* **2000**, *112*, 3676–3701; *Angew. Chem. Int. Ed.* **2000**, *39*, 3532–3556; b) K. Mikami, M. Terada, T. Korenaga, Y. Matsumoto, S. Matsukawa, *Acc. Chem. Res.* **2000**, *33*, 391–401; For more recent reviews, see; c) K. Mikami, M. Yamanaka, *Chem. Rev.* **2003**, *103*, 3369–3400; d) J. W. Faller, A. R. Lavoie, J. Parr, *Chem. Rev.* **2003**, *103*, 3345–3367.

[6] For leading examples of asymmetric activation, see: a) K. Mikami, S. Matsukawa, *Nature* **1997**, *385*, 613–615; b) K. Mikami, S. Matsukawa, T. Volk, M. Terada, *Angew. Chem.* **1997**, *109*, 2936–2939; *Angew. Chem. Int. Ed. Engl.* **1997**, *36*, 2768–2771; c) T. Ohkuma, H. Doucet, T. Pham, K. Mikami, T. Korenaga, M. Terada, R. Noyori, *J. Am. Chem. Soc.* **1998**, *120*, 1086–1087; d) K. Mikami, T. Korenaga, T. Ohkuma, R. Noyori, *Angew. Chem.* **2000**, *112*, 3854–3857; *Angew. Chem. Int. Ed.* **2000**, *39*, 3707–3710; e) A. Ishii, V. A. Soloshonok, K. Mikami, *J. Org. Chem.* **2000**, *65*, 1597–1599; f) K. Mikami, K. Aikawa, Y. Yusa, *Org. Lett.* **2002**, *4*, 95–97; g) K. Mikami, K. Aikawa, T. Korenaga, *Org. Lett.* **2001**, *3*, 243–245; h) K. Mikami, K. Aikawa, *Org. Lett.* **2002**, *4*, 99–101; i) J. Hao, M. Hatano, K. Mikami, *Org. Lett.* **2000**, *2*, 4059–4062; j) K. Mikami, K. Aikawa, Y. Yusa, M. Hatano, *Org. Lett.* **2002**, *4*, 91–94; k) K. Ding, A. Ishii, K. Mikami, *Angew. Chem.* **1999**, *111*, 519–523; *Angew. Chem. Int. Ed.* **1999**, *38*, 497–501; l) K. Mikami, R. Angelaud, K. Ding, A. Ishii, A. Tanaka, N. Sawada, K. Kudo, M. Senda, *Chem. Eur. J.* **2001**, *7*, 730–737; m) K. Mikami, H. Kakuno, K. Aikawa, *Angew. Chem.* **2005**, *117*, 7423–7426; *Angew. Chem. Int. Ed.* **2005**, *44*, 7257–7260; n) K. Mikami, S. Kataoka, K. Aikawa, *Org. Lett.* **2005**, *7*, 5777–5780; o) T. Korenaga, K. Aikawa, M. Terada, S. Kawauchi, K. Mikami, *Adv. Synth. Catal.* **2001**, *343*, 284–288; p) K. Aikawa, K. Mikami, *Angew. Chem.* **2003**, *115*, 5613–5616; *Angew. Chem. Int. Ed.* **2003**, *42*, 5455–5458; q) K. Aikawa, K. Mikami, *Angew. Chem.* **2003**, *115*, 5616–5619; *Angew. Chem. Int. Ed.* **2003**, *42*, 5458–5461.

[7] a) K. Mikami, T. Korenaga, M. Terada, T. Ohkuma, T. Pham, R. Noyori, *Angew. Chem.* **1999**, *111*, 517–519; *Angew. Chem. Int. Ed.* **1999**, *38*, 495–497; b) M. Yamanaka, K. Mikami, *Organometallics* **2002**, *21*, 5847–5851.

[8] During the preparation of this manuscript, Mikami et al. independently reported the use of **3a** for efficient hydrogenation of a number of aryl ketones: K. Mikami, K. Wakabayashi, K. Aikawa, *Org. Lett.* **2006**, *8*, 1517–1519.

[9] Benzophenone crystallizes in chiral space group $P2_12_12_1$, see: a) E. B. Fleischer, N. Sung, S. Hawkinson, *J. Phys. Chem.* **1968**, *72*, 4311–4312; b) H. Koshima, *Kokagaku* **1996**, *3*, 64–65; c) T. Matsuura, H. Koshima, *J. Photochem. Photobiol. C Photochem. Rev.* **2005**, *6*, 7–24.

[10] a) C. Faerman, H. Negri, G. Punte, A. A. Vitale, N. S. Nudelman, *Can. J. Chem.* **1983**, *61*, 2001–2005; b) T. Yamato, H. Inoue, K. Maeda, M. Tashiro, *J. Chem. Res. (M)* **1996**, *7*, 1731–1745.

[11] a) W. Liu, *Synth. Commun.* **1997**, *27*, 3701–3704; b) U. Verkerk, M. Fujita, T. L. Dzwiniel, R. McDonald, J. M. Stryker, *J. Am. Chem. Soc.* **2002**, *124*, 9988–9989.

[12] a) P. R. Brooks, M. C. Wirtz, M. G. Vetelino, D. M. Rescek, G. F. Woodworth, B. P. Morgan, J. W. Coe, *J. Org. Chem.* **1999**, *64*, 9719–9721; b) W. M. Horspool, P. L. Pauson, *J. Chem. Soc.* **1965**, 5162–5164.

[13] D. Cai, J. F. Payack, D. R. Bender, D. L. Hughes, T. R. Verhoeven, P. J. Reider, *J. Org. Chem.* **1994**, *59*, 7180–7181.

[14] Q. Jing, X. Zhang, J. Sun, K. Ding, *Adv. Synth. Catal.* **2005**, *347*, 1193–1197.

[15] The reaction rate was found to increase significantly with increasing H_2 pressure: 57% conversion, $p(H_2)$ = 10 atm, t = 4 h, Table 2; ca. 75% conversion, $p(H_2)$ = 15 atm, t = 4 h, Figure 2,

a; >99% conversion, $p(H_2)$ = 20 atm, t = 3 h, Table S1 in the Supporting Information.
[16] Mikami et al. reported that the hydrogenation of **21** with the analogous catalyst containing reduced **9a** (DPBOL) ligand gives the corresponding secondary alcohol in 66% *ee*; see ref.[8]
[17] a) B. Andersh, D. L. Murphy, R. J. Olson, *Synth. Commun.* **2000**, *30*, 2091–2098; b) W. K. Warren, *J. Org. Chem.* **1961**, *26*, 4851–4855; c) K. M. Alok, D. Aparna, K. Nilay, *Indian J. Chem., B* **2000**, *39*, 387–389.
[18] I. Masaaki, E. Sakae, *Bull. Chem. Soc. Jpn.* **1974**, *47*, 1687–1692.

Received: April 6, 2006
Published Online: June 19, 2006

